agriculture

MDPI

Article

Soil Water–EC Dynamics and Soil–Crop Responses to Organic Fertiliser and *Bacillus subtilis* Rates Under Magnetised–Ionised Water Irrigation in a Saline–Alkali Cotton Field

Haichao Wang [1,2], Zhenghu Ma [1,2], Yan Xu [3], Qiuping Fu [1,2,*], Shudong Lin [1,2,*], Zhen Shen [1,2], Yongji Zhou [1,2], Qingshu Ma [1,2], Yingjie Ma [1,2] and Quanjiu Wang [4]

[1] College of Hydraulic and Civil Engineering, Xinjiang Agricultural University, Urumqi 830052, China
[2] Xinjiang Key Laboratory of Hydraulic Engineering Security and Water Disasters Prevention, Urumqi 830052, China
[3] Eco-Hydraulic Research Center of the Xinjiang Uygur Autonomous Region (Academician and Expert Workstation, Department of Water Resources of the Xinjiang Uygur Autonomous Region), Urumqi 830015, China
[4] State Key Laboratory of Water Engineering Ecology and Environment in Arid Area, Xi'an University of Technology, Xi'an 710048, China
* Correspondence: qiupingfu@xjau.edu.cn (Q.F.); shudong_lin@163.com (S.L.)

Abstract

Amendment studies in saline–alkali cropland often emphasise treatment–control comparisons, whereas rate-dependent responses within the same field system remain less well resolved. We evaluated water-soluble organic fertiliser and *Bacillus subtilis* rates in a saline–alkali cotton (*Gossypium hirsutum* L.) field under magnetised–ionised water irrigation. A single-season (2025) randomised complete block experiment with three replicates included CK1 (magnetised–ionised water without amendments), CK2 (conventional water without amendments), and a 3 × 3 factorial of organic fertiliser (300, 600, and 900 kg ha^{-1}) and inoculant (30, 52.5, and 75 kg ha^{-1}) rates. Gravimetric soil water content (GSWC) and electrical conductivity (EC) were measured across five growth stages and seven soil layers; post-harvest bulk density, boll-stage microbial composition, leaf gas exchange, and seed cotton yield were also assessed. GSWC and EC showed stage- and depth-dependent responses. Post-harvest bulk density showed a non-monotonic pattern across organic fertiliser rates. Y2W2 produced the highest observed net photosynthetic rate and seed cotton yield, 14.04% and 10.51% above CK1, respectively, and the lowest observed bulk density at both depths, 2.84–4.00% below CK1. Mantel analysis indicated positive covariation of bacterial assemblage composition with boll-stage GSWC and seed cotton yield, although statistical support was limited after multiple-testing correction. Y2W2 showed favourable responses across several indicators but requires multi-season and multi-site validation.

Keywords: gravimetric soil water content; electrical conductivity; microbial assemblage; dose response; drip irrigation; soil bulk density

Check for updates

Received: 3 September 2026
Revised: 8 October 2026
Accepted: 13 October 2026
Published: 28 October 2026

Copyright: © 2026 by the authors. Licensee MDPI, Basel, Switzerland. This article is an open access article distributed under the terms and conditions of the Creative Commons Attribution (CC BY) license.

1. Introduction

Saline–alkali soils impose multiple and concurrent constraints on crop production, including restricted soil water availability, accumulation of soluble salts, deterioration of soil physical condition, and impaired nutrient cycling [1]. These constraints are particularly important in arid irrigated regions, where root-zone water and salt distributions are strongly influenced by irrigation and evaporation. Cotton is an agronomically important crop in

southern Xinjiang, where film-mulched drip irrigation is widely used under conditions of water scarcity and salinity risk [2–4]. Cotton was therefore studied here as the principal crop of this salt-affected production system rather than as an arbitrary model species, and the findings are specific to it. Organic amendments, microbial inoculants, and modified irrigation water have therefore been investigated as complementary approaches to improve soil conditions and sustain crop production in salt-affected agroecosystems [4–6]. Previous studies further indicate that responses to organic amendments and *Bacillus subtilis* can vary with application rate rather than simply with amendment presence [5–8]. However, whether such rate-related responses are expressed consistently across soil, microbial, and crop components within the same field system remains less well understood.

Soil water content and electrical conductivity (EC) are particularly dynamic under drip irrigation. Their distributions reflect the combined effects of irrigation, evapotranspiration, redistribution, and leaching, and consequently vary during the growing season and through the soil profile [2,9]. Amendment-rate responses may therefore emerge in particular soil layers or developmental periods rather than uniformly throughout the profile. Layer-specific analysis is needed to identify where these responses occur, whereas cumulative-profile summaries can provide complementary information on whether treatment differences remain evident when progressively deeper soil is integrated. Because cumulative profiles are nested rather than independent, they are considered here as integrated descriptive summaries rather than independent spatial scales.

Magnetised–ionised water may further modify the physicochemical context in which amendments are applied. Magnetic and ionisation treatments have been reported to alter water properties such as hydrogen-bond organisation, surface tension, and ion behaviour; lower surface tension and weaker molecular association are hypothesised to improve soil wetting and infiltration, and thereby to favour the dissolution and leaching of salts and the dissolution and delivery of water-soluble amendments [10–14]. However, the magnitude and persistence of these effects depend on treatment conditions and water chemistry, and their reproducibility varies among experimental systems [13]. In the present experiment, magnetised–ionised water therefore served as the common irrigation background for evaluating organic fertiliser and inoculant rates, while CK1 and CK2 provided a reference comparison between magnetised–ionised and conventional irrigation in the absence of amendments. Organic fertiliser and microbial inoculation may also influence soil and crop responses through processes that do not necessarily parallel changes in EC. Organic inputs can alter resource availability and soil structural condition, whereas microbial inoculation can influence rhizosphere resource turnover and other biological processes [15,16]. Soil microbial assemblages constitute an additional biological component of amendment response, and bacterial and fungal communities may show distinct compositional responses to changes in organic resource supply and soil environmental conditions [17–19]. Because amplicon sequencing characterises relative taxonomic composition rather than microbial function, the microbial results are interpreted as compositional responses and covariation rather than direct evidence of microbial mediation. The boll stage was selected for microbial and leaf gas-exchange measurements because it represents an active reproductive period in cotton during which water supply and photosynthetic carbon assimilation are closely related to boll development and subsequent yield formation [20].

Previous field studies in southern Xinjiang have examined *B. subtilis* application rates under magnetised–ionised irrigation and the combined use of magnetised–ionised water and organic fertilisation [5,8,10]. These studies indicate that soil and crop responses can be rate-dependent and non-linear. What remains less well resolved is how simultaneous variation in organic fertiliser and microbial inoculant rates is expressed across seasonal soil water–salt dynamics, post-harvest soil physical condition, microbial assemblages, crop

physiology, and yield within the same field experiment. Evaluating these components together can clarify whether amendment-rate responses are broadly coordinated across the soil–microbe–crop system or instead depend on growth stage, soil depth, input factor, or crop trait.

Accordingly, we crossed three rates of water-soluble organic fertiliser with three rates of *B. subtilis* inoculant under a common magnetised–ionised water irrigation background. Gravimetric soil water content (GSWC) and EC were monitored at five growth stages across seven measured soil layers, with cumulative-profile values retained as complementary integrated summaries. Bacterial and fungal family composition and leaf gas exchange were characterised at the boll stage, post-harvest bulk density was assessed as a soil physical endpoint, and seed cotton yield and its components represented final agronomic responses. We addressed three questions: (1) whether the effects of organic fertiliser rate, inoculant rate, and their interaction on GSWC and EC vary with growth stage and soil depth, and how the two variables differ in effect magnitude and detection precision; (2) whether bacterial and fungal assemblages and family-level composition respond to amendment rates and covary with concurrent soil and crop conditions at the boll stage; and (3) whether post-harvest bulk density, boll-stage leaf gas exchange, and final yield and yield components exhibit factor-specific, combination-dependent, or non-linear responses within the tested rate range rather than a uniform proportional response to increasing input.

2. Materials and Methods

2.1. Site, Experimental Design, and Field Management

The experiment was conducted from April to September 2025 at Gongqingtuan Town, Wensu County, Aksu Prefecture, Xinjiang, China (80°39′38″ E, 41°8′52″ N). The site has an arid continental climate, with a mean annual temperature of 10.1 °C, mean annual precipitation of 65.4 mm, and a frost-free period of approximately 185 d. Meteorological conditions during the 2025 experimental period, including air temperature and precipitation, are shown in Figure 1. The soil texture was sandy loam. Before treatment establishment, the 0–20 cm soil layer had a bulk density of 1.53 g cm^{-3}, pH of 8.10, electrical conductivity (EC; 1:5 soil-to-water extract) of 1.72 mS cm^{-1}, and soil organic matter content of 8.57 g kg^{-1}. Total N, P, and K concentrations were 0.88, 0.79, and 21.88 g kg^{-1}, respectively, and alkali-hydrolysable N, available P, and available K concentrations were 23.59, 21.17, and 112.28 mg kg^{-1}, respectively. These baseline soil properties were determined using standard agrochemical methods [21]. The field is referred to as saline–alkali on the basis of its EC and alkaline pH; exchangeable sodium percentage (ESP) and sodium adsorption ratio (SAR) were not determined.

Cotton cultivar ‘Xinluzhong 82’ was sown on 14 April and harvested on 26 September 2025. Cotton was planted using the locally adopted machine-harvest configuration of one plastic-mulch strip, three sub-mulch drip lines, and six cotton rows. Eleven treatments were arranged in a randomised complete block design with three blocks. Each treatment occurred once within each block in a 45 m^2 plot, giving 33 plots in total; the plot was the experimental unit for all measurements and analyses reported in this study. Treatments comprised conventional-water irrigation without organic fertiliser or microbial inoculant (CK2), magnetised–ionised water irrigation without either amendment (CK1), and nine Y1W1–Y3W3 combinations of three water-soluble organic fertiliser rates (Y1, 300; Y2, 600; and Y3, 900 kg ha^{-1}) and three *Bacillus subtilis* inoculant rates (W1, 30; W2, 52.5; and W3, 75 kg ha^{-1}), all under magnetised–ionised water irrigation.

Irrigation-water type was not fully crossed with organic fertiliser and inoculant rate. Accordingly, factorial effects of organic fertiliser rate, inoculant rate, and their interaction were estimated specifically within the magnetised–ionised water irrigation background.

CK1 and CK2 provided a reference comparison between conventional and magnetised–ionised water irrigation in the absence of either amendment, but this contrast does not estimate interactions between irrigation-water type and amendment rate.

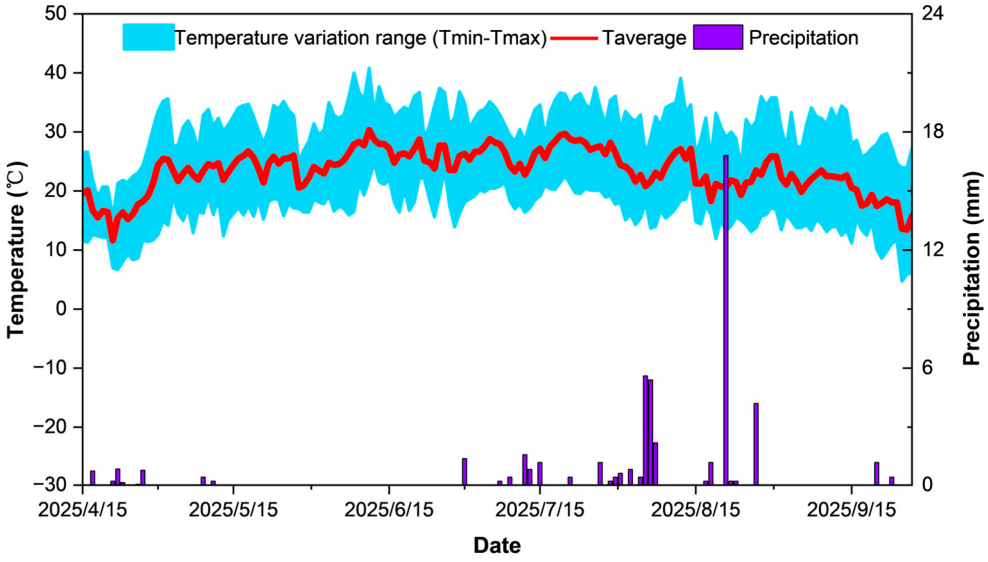


Figure 1. Daily temperatures and rainfall during the 2025 cotton season.

Magnetised–ionised water was produced with a BI-DM902 magnetoelectric activation device (Xi'an University of Technology, Xi'an, China) at a magnetic flux density of 3000 G. The device was installed on a 90 mm-diameter pipe connected to the outlet of the main irrigation pipeline. Water passing through the device was applied directly to the field without intermediate storage. Irrigation volume was metered independently for each plot using individual water meters. Conventional water for CK2 was supplied through a separate branch line upstream of the magnetoelectric activation device, whereas magnetised–ionised water was delivered through a separate downstream line after treatment by the device to CK1 and the nine factorial amendment treatments. Plot-level water meters were used to control irrigation volumes independently. Buffer rows were established between plots receiving conventional and magnetised–ionised water to minimise lateral water movement between the two irrigation-water treatments. The water-soluble organic fertiliser had a manufacturer-declared composition of ≥40% organic matter, ≥10% amino acids, ≥5% fulvic acid, and ≥5% total N + P_2O_5 + K_2O (Chengdu Huahong Biotechnology, Chengdu, China). The inoculant was a *B. subtilis* wettable powder containing ≥ 1.0×10^{11} viable CFU g^{-1} (Baoding Kelüfeng Biochemical Technology, Baoding, China). On the basis of the declared composition, the organic fertiliser also supplied at least 15, 30, and 45 kg ha^{-1} of N + P_2O_5 + K_2O at Y1, Y2, and Y3, respectively; the soluble-salt content of the two commercial products and the composition of the inoculant carrier were not determined. All treatments received an identical irrigation schedule of 465 mm in 12 events. Organic fertiliser and inoculant were delivered through a differential-pressure fertiliser tank with the irrigation water, each treatment's total being divided into six equal doses applied during irrigation events 4–9. Chemical fertiliser, pest, weed and disease control, growth regulation, and topping were identical across plots and followed local high-yield machine-harvest practice.

2.2. Seasonal and Depth-Resolved Measurements of Gravimetric Soil Water Content and Electrical Conductivity

Soil was sampled at five growth stages (seedling, squaring, flowering, boll formation, and boll opening) from seven depth intervals (0–10, 10–20, 20–30, 30–40, 40–60, 60–80, and

80–100 cm). Seedling-stage sampling was conducted 3 d after the third irrigation event, whereas sampling at the squaring, flowering, boll-formation, and boll-opening stages was conducted 4 d after the most recent irrigation event.

At each depth interval, samples were collected separately from three predefined lateral zones within each plot, representing the wide-row, narrow-row, and bare-soil zones. At each sampling event, new sampling points were selected within the same predefined lateral zones to avoid previously disturbed locations, and sampling holes were backfilled after collection.

Gravimetric soil water content (GSWC) was determined by oven-drying soil samples at 105 °C to constant mass and was expressed on a dry-soil mass basis (g g^{-1}). Electrical conductivity (EC) was measured in a 1:5 soil-to-water extract using a conductivity meter.

2.3. Post-Harvest Soil Bulk Density

Immediately after mechanical harvesting, one undisturbed soil core was collected from each of the 0–20 and 20–40 cm layers in every plot using 100 cm^3 core rings. Sampling positions were located directly beneath cotton plants and outside visible machinery wheel tracks. For the 0–20 and 20–40 cm soil layers, ring-core samples were collected from the middle portion of each layer, corresponding to approximately 6–14 cm and 26–34 cm soil depth, respectively. The cores were oven-dried at 105 °C to constant mass, and soil bulk density was calculated from oven-dry soil mass and core volume. Because each treatment was represented by one plot in each of the three blocks, three independent plot-level observations were obtained per treatment at each soil depth for statistical analysis. The pre-sowing bulk-density value reported in Section 2.1 was used only to characterise the initial soil condition and was not treated as a paired pre- and post-treatment observation.

2.4. Bacterial and Fungal Family Composition

At the boll stage, soil samples were collected from the 0–20 cm layer in the narrow-row zone of each plot using a five-point sampling scheme. The five subsamples from each plot were combined, and visible stones, roots and plant residues were removed before thorough homogenisation to form one composite sample, yielding 33 plot-level samples in total. Samples were preserved on dry ice immediately after collection until DNA extraction.

Microbial genomic DNA was extracted using the E.Z.N.A.® Soil DNA Kit (Omega Biotek, Norcross, GA, USA). DNA quality and integrity were checked by 1% agarose gel electrophoresis. The bacterial 16S rRNA V3–V4 region was amplified using the primer pair 341F (5′-CCTAYGGGRBGCASCAG-3′) and 806R (5′-GGACTACNNGGGTATCTAAT-3′), while the fungal ITS1 region was amplified using the primer pair ITS1F (5′-CTTGGTCATTTAGAGGAAGTAA-3′) and ITS2R (5′-GCTGCGTTCTTCATCGATGC-3′). PCR reactions were performed in triplicate using TransStart FastPfu DNA Polymerase (TransGen Biotech, Beijing, China). Purified amplicons were pooled at equimolar concentrations and subjected to paired-end sequencing (2 × 300 bp) by Shanghai Biozeron Biotechnology Co., Ltd. (Shanghai, China).

Raw reads were demultiplexed according to sample-specific barcodes and primer sequences, followed by quality filtering, paired-end merging, chimera removal, and denoising. Reads were trimmed using a 10 bp sliding window at Q20, reads < 50 bp were discarded, barcode mismatches were not allowed, and up to two primer mismatches were permitted. Paired reads with >10 bp overlap were merged and chimeras removed. Amplicon sequence variants (ASVs) were generated using DADA2. After quality filtering and sequence processing, 55,178–64,254 valid sequences per sample (mean 59,755) were retained for the 16S rRNA gene dataset and 49,065–64,702 (mean 53,828) for the ITS dataset. Bacterial representative sequences were taxonomically assigned against SILVA SSU 138.1 and fungal sequences against NT-fungi v202307. Subsequent analyses focused on family-level composi-

tion, represented by the 20 dominant families and an aggregated Other category. The raw 16S rRNA gene and ITS sequencing data have been deposited in the NCBI Sequence Read Archive under BioProject accession number PRJNA1513417.

2.5. Leaf Gas Exchange, Yield, and Yield Components

Leaf gas exchange was measured at the boll stage on 3 August 2025 between 12:00 and 14:00 Beijing Time (UTC+8; approximately 09:20–11:20 local solar time at the site longitude) using a CIRAS-3 portable photosynthesis system (PP Systems, Amesbury, MA, USA). The daily mean and maximum air temperatures on 3 August were 21.6 and 31.8 °C, respectively (Figure 1). One representative plant was randomly selected from each plot, resulting in three plants per treatment and 33 measurements in total. One measurement was taken from the third fully expanded main-stem leaf from the apex after the gas-exchange variables had stabilised. Net photosynthetic rate (Pn), transpiration rate (Tr), stomatal conductance (Gs), and intercellular CO_2 concentration (Ci) were recorded. Cuvette conditions (PPFD, reference CO_2 concentration, leaf temperature, and vapour-pressure deficit) and the order in which plots were measured were not documented in the retained records; the gas-exchange data are therefore interpreted as relative differences among treatments under the conditions prevailing on that date.

Yield was determined from one 2 m × 2 m quadrat in each plot, the plot again being the replicate [3]. The quadrat was located in an area of uniform and representative crop growth within each plot, excluding border rows, plot ends, and buffer zones. Mature bolls were hand-harvested, and seed cotton mass was expressed per unit area; plant and boll counts from the same quadrat gave bolls per plant; 100 randomly sampled mature bolls per plot gave 100-boll weight.

2.6. Statistical Analysis

For each soil layer and sampling event, gravimetric soil water content (GSWC) and electrical conductivity (EC) measured in the wide-row, narrow-row, and bare-soil zones were combined to obtain plot-level values using area-weighted means. The three zones represented 132, 58, and 30 cm, respectively, of each 220 cm transverse planting unit, corresponding to weights of 0.60000, 0.2636, and 0.1364. For descriptive cumulative-profile summaries, these area-weighted layer-specific values were further combined according to layer thickness to derive thickness-weighted means for the nested 0–20, 0–40, 0–60, and 0–100 cm profiles. Because these cumulative profiles are inherently nested and non-independent, they were used only as integrated descriptive summaries and not as independent inferential scales. Amendment application began with the fourth irrigation; therefore, the corresponding seedling-stage value for each plot and soil layer was used as the pre-amendment covariate in subsequent analyses. Formal statistical inference was based on the seven directly measured soil layers, with the plot treated as the experimental unit.

Within the nine Y1W1–Y3W3 combinations, post-amendment GSWC and EC were analysed by soil layer using baseline-adjusted repeated-stage generalised least-squares (GLS) models with Y, W, Stage, and their interactions as fixed effects, block included as a fixed blocking factor, and plot treated as the repeated-measures subject across the four post-amendment stages. Temporal covariance structures were selected by AIC from IID, compound-symmetry (CS), and unstructured (UN) candidates. A discrete first-order autoregressive [AR(1)] structure based on growth-stage order was additionally evaluated as a diagnostic alternative; because the intervals among the four post-amendment sampling stages were unequal, AR(1) was not included in the formal covariance-structure selection (Table S1). Omnibus stage interactions were followed by stage-specific Y, W, and Y × W tests, with BH adjustment across the 28 stage × depth tests within each effect and response

variable. Depth and its interactions with Y, W, and Y × W were also tested separately at each post-amendment stage. Partial ηp^2 with 95% confidence intervals, residual CV, and relative MDD80 were used to characterise effect magnitude and detection precision. MDD80 was the minimum detectable difference between two treatment-cell means at $\alpha = 0.05$ and 80% power, assuming three replicates per cell; relative MDD80 was expressed as a percentage of the corresponding mean response. Planned contrasts compared CK1 with CK2 and the mean of the nine Y1W1–Y3W3 combinations with CK1, with BH adjustment applied within contrast families. The CK1–CK2 contrast used all five stages without baseline adjustment, whereas the factorial-mean–CK1 contrast used the four post-amendment stages with seedling-stage baseline adjustment.

Microbial analyses used the 20 most abundant bacterial or fungal families plus an aggregated Other category. Compositions were CLR-transformed, with multiplicative zero replacement applied to fungal data where required. Assemblage-level treatment, Y, W, and Y × W effects were tested using block-restricted PERMANOVA with 9999 permutations. Family-level models included block as a blocking factor, with p values obtained from 9999 within-block permutations and BH-FDR correction applied across 80 tests (20 named families × four effects) within each microbial domain. The Other category was included in the CLR transformation and assemblage-level PERMANOVA but excluded from family-specific tests.

Post-harvest bulk density, boll-stage gas-exchange traits, seed cotton yield, and yield components were analysed at the plot level. For all 11 treatments, treatment and block were included in the model, and means were separated by Duncan's multiple range test at $p < 0.05$; factorial inference and planned dose contrasts were restricted to the nine Y1W1–Y3W3 treatments. Within the nine Y1W1–Y3W3 combinations, Y, W, and Y × W effects were tested together with orthogonal linear and quadratic contrasts and planned adjacent-level comparisons, followed by BH adjustment. Exploratory response-surface models included CK1 as the zero-input point and excluded CK2, and were used only to characterise response curvature.

Spearman correlations among boll-stage soil, gas-exchange, and yield-related variables were calculated from the 33 plot-level observations, with BH adjustment across 36 pairwise tests. Mantel tests assessed covariation between dominant-family assemblage composition and individual soil or crop variables using Aitchison distances, 9999 permutations restricted within block, and BH adjustment across 18 tests. Post-harvest bulk density was excluded from these association analyses. Significance was assessed at $q < 0.05$ for multiplicity-adjusted analyses and otherwise at $p < 0.05$. Statistical analyses were performed mainly in Python 3.12.14 using NumPy 2.3.5, pandas 3.0.1, and SciPy 1.18.1, with complementary analyses conducted in SPSS 27.0. Figures were prepared in Python and Origin 2024.3.

3. Results

3.1. Seasonal and Depth-Resolved Responses of GSWC and EC

GSWC and EC exhibited pronounced variation with growth stage and soil depth (Figures 2 and 3). Baseline-adjusted analyses showed significant Y × Stage and Y × W × Stage interactions for both variables at all seven measured depths, except for the Y × Stage interaction for EC at 0–10 cm. The W × Stage effect was significant at all depths for GSWC, whereas for EC it was significant at 10–100 cm but not at 0–10 cm. In addition, Depth and its interactions with Y, W, and Y × W were significant at all post-amendment stages ($p < 0.05$; Tables 1 and S2), indicating clear stage- and depth-dependent treatment responses.

Table 1. Baseline-adjusted stage-dependent effects of organic fertiliser and inoculant rates on GSWC and EC.

Variable	Depth (cm)	Y × Stage	W × Stage	Y × W × Stage
GSWC	0–10	$F(6, 69) = 5.041$; $p = 0.0002$; $\eta p^2 = 0.305$	$F(6, 69) = 18.032$; $p < 0.0001$; $\eta p^2 = 0.611$	$F(12, 69) = 10.551$; $p < 0.0001$; $\eta p^2 = 0.647$
GSWC	10–20	$F(6, 69) = 3.910$; $p = 0.0020$; $\eta p^2 = 0.254$	$F(6, 69) = 22.561$; $p < 0.0001$; $\eta p^2 = 0.662$	$F(12, 69) = 5.005$; $p < 0.0001$; $\eta p^2 = 0.465$
GSWC	20–30	$F(6, 69) = 7.681$; $p < 0.0001$; $\eta p^2 = 0.400$	$F(6, 69) = 33.916$; $p < 0.0001$; $\eta p^2 = 0.747$	$F(12, 69) = 11.514$; $p < 0.0001$; $\eta p^2 = 0.667$
GSWC	30–40	$F(6, 69) = 21.651$; $p < 0.0001$; $\eta p^2 = 0.653$	$F(6, 69) = 55.466$; $p < 0.0001$; $\eta p^2 = 0.828$	$F(12, 69) = 5.011$; $p < 0.0001$; $\eta p^2 = 0.466$
GSWC	40–60	$F(6, 69) = 31.992$; $p < 0.0001$; $\eta p^2 = 0.736$	$F(6, 69) = 56.733$; $p < 0.0001$; $\eta p^2 = 0.831$	$F(12, 69) = 20.435$; $p < 0.0001$; $\eta p^2 = 0.780$
GSWC	60–80	$F(6, 69) = 32.507$; $p < 0.0001$; $\eta p^2 = 0.739$	$F(6, 69) = 17.409$; $p < 0.0001$; $\eta p^2 = 0.602$	$F(12, 69) = 34.028$; $p < 0.0001$; $\eta p^2 = 0.855$
GSWC	80–100	$F(6, 69) = 58.999$; $p < 0.0001$; $\eta p^2 = 0.837$	$F(6, 69) = 13.638$; $p < 0.0001$; $\eta p^2 = 0.543$	$F(12, 69) = 12.527$; $p < 0.0001$; $\eta p^2 = 0.685$
EC	0–10	$F(6, 69) = 1.614$; $p = 0.1560$; $\eta p^2 = 0.123$	$F(6, 69) = 1.740$; $p = 0.1250$; $\eta p^2 = 0.131$	$F(12, 69) = 3.234$; $p = 0.0010$; $\eta p^2 = 0.360$
EC	10–20	$F(6, 69) = 5.488$; $p = 0.0001$; $\eta p^2 = 0.323$	$F(6, 69) = 3.204$; $p = 0.0080$; $\eta p^2 = 0.218$	$F(12, 69) = 5.641$; $p < 0.0001$; $\eta p^2 = 0.495$
EC	20–30	$F(6, 69) = 16.836$; $p < 0.0001$; $\eta p^2 = 0.594$	$F(6, 69) = 14.922$; $p < 0.0001$; $\eta p^2 = 0.565$	$F(12, 69) = 9.145$; $p < 0.0001$; $\eta p^2 = 0.614$
EC	30–40	$F(6, 69) = 25.999$; $p < 0.0001$; $\eta p^2 = 0.693$	$F(6, 69) = 18.564$; $p < 0.0001$; $\eta p^2 = 0.617$	$F(12, 69) = 18.114$; $p < 0.0001$; $\eta p^2 = 0.759$
EC	40–60	$F(6, 69) = 13.227$; $p < 0.0001$; $\eta p^2 = 0.535$	$F(6, 69) = 4.816$; $p = 0.0004$; $\eta p^2 = 0.295$	$F(12, 69) = 15.390$; $p < 0.0001$; $\eta p^2 = 0.728$
EC	60–80	$F(6, 69) = 21.084$; $p < 0.0001$; $\eta p^2 = 0.647$	$F(6, 69) = 2.523$; $p = 0.0290$; $\eta p^2 = 0.180$	$F(12, 69) = 12.247$; $p < 0.0001$; $\eta p^2 = 0.681$
EC	80–100	$F(6, 69) = 42.213$; $p < 0.0001$; $\eta p^2 = 0.786$	$F(6, 69) = 81.447$; $p < 0.0001$; $\eta p^2 = 0.876$	$F(12, 69) = 43.023$; $p < 0.0001$; $\eta p^2 = 0.882$

For Y × Stage and W × Stage, $df = 6, 69$; for Y × W × Stage, $df = 12, 69$. Effect sizes are reported as partial eta squared (η_p^2). Y, organic fertiliser rate; W, microbial inoculant rate; Stage, cotton growth stage.

For GSWC, treatment differences were particularly evident during boll formation and boll opening (Figure 2). At boll formation, across the 0–30 cm layers for which the corresponding baseline-adjusted contrasts were significant ($q < 0.05$), the observed mean GSWC of the nine factorial treatments was 11.1–35.4% higher than that of CK1, with the largest increase occurring at 10–20 cm. At the same stage, only the CK1–CK2 contrast at 60–80 cm remained significant after multiple-testing adjustment. At boll opening, the observed mean GSWC of the nine factorial treatments was 12.1–31.4% higher than CK1 across 0–40 cm, with significant baseline-adjusted contrasts in all four layers.

For EC, the clearest treatment differences occurred during boll formation (Figure 3). Across the six soil layers for which the corresponding baseline-adjusted contrasts were significant ($q < 0.05$), the observed mean EC of the nine factorial treatments was 16.7–38.8% lower than CK1, with significant differences extending from 0–10 to 60–80 cm. The largest reductions occurred at 30–40 and 40–60 cm, reaching 37.4% and 38.8%, respectively. In contrast, none of the layer-specific CK1–CK2 contrasts at boll formation remained significant after Benjamini–Hochberg adjustment. At boll opening, EC remained significantly lower than CK1 at 0–10, 10–20, and 30–40 cm, with observed reductions of 17.2–17.5% (Table S3).

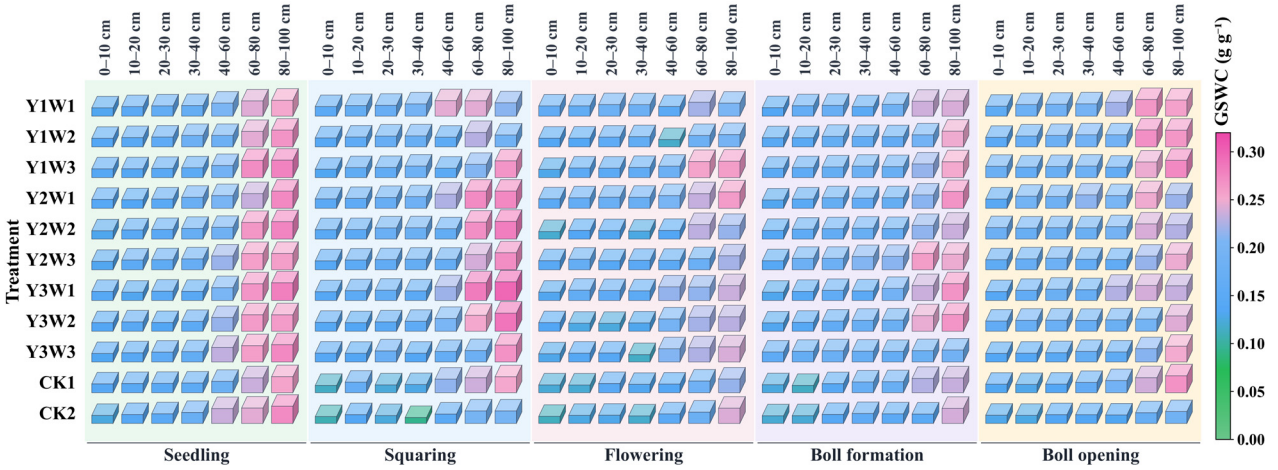


Figure 2. Seasonal and depth-resolved variation in gravimetric soil water content (GSWC) across the 11 treatments at key cotton growth stages. Each prism represents the treatment mean of three independent plots ($n = 3$).

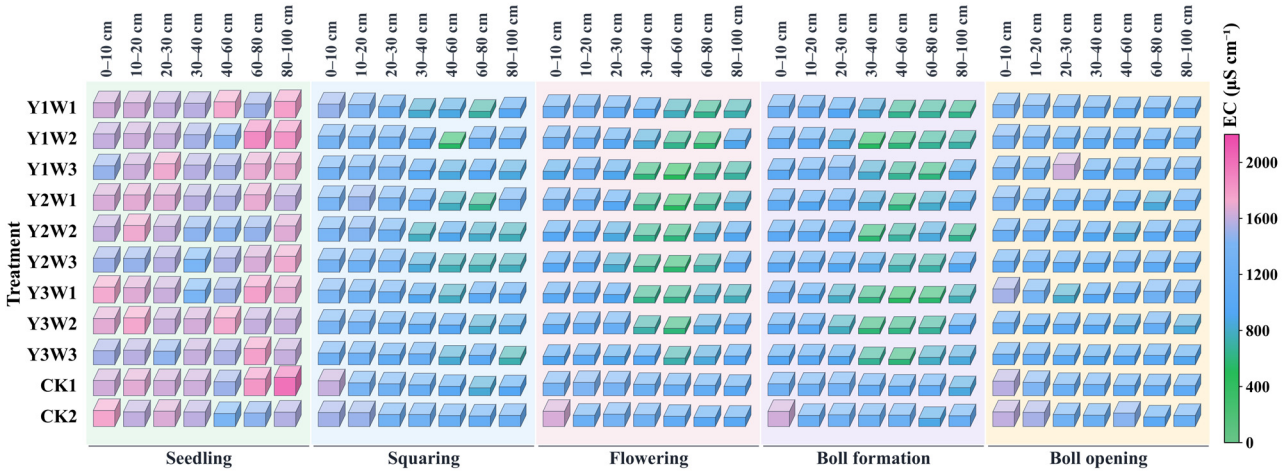


Figure 3. Seasonal and depth-resolved variation in soil electrical conductivity (EC) across the 11 treatments at key cotton growth stages. Each prism represents the treatment mean of three independent plots ($n = 3$).

Differences between GSWC and EC were more evident in detection precision than in overall standardised effect magnitude. Median partial η_p^2 values for Y were broadly comparable between GSWC and EC, as were those for Y × W, whereas the W effect was larger for GSWC. GSWC also showed lower residual CV and relative MDD_{80} than EC, indicating greater detection precision under the present experimental design (Table 2).

As a complementary integrated view, the nested 0–20, 0–40, 0–60, and 0–100 cm profiles retained the main seasonal patterns observed in the layer-specific analyses (Figure 4). During boll formation and boll opening, the nine Y1W1–Y3W3 combinations generally showed higher GSWC and lower EC than CK1, while CK1 also tended to show higher GSWC and lower EC than CK2. The magnitude of these differences varied with cumulative profile depth. Because the nested profiles share constituent soil layers and are statistically non-independent, they are presented only as complementary descriptive summaries rather than as independent inferential scales.

Table 2. Standardised effect magnitude and detection precision of GSWC and EC after baseline adjustment.

Variable	Y Partial ηp^2, Median (IQR)	W Partial ηp^2, Median (IQR)	Y × W Partial ηp^2, Median (IQR)	Residual CV, Median (IQR), %	Relative MDD80, Median (IQR), %
GSWC	0.511 (0.236–0.665)	0.591 (0.328–0.790)	0.610 (0.441–0.733)	5.095 (4.335–5.936)	12.368 (10.523–14.410)
EC	0.553 (0.473–0.646)	0.390 (0.198–0.617)	0.596 (0.403–0.776)	7.491 (5.904–8.892)	18.184 (14.332–21.586)

Values are medians (interquartile ranges, IQRs) across the four post-amendment growth stages and seven measured soil layers. η_p^2, partial eta squared; CV, coefficient of variation; MDD80, minimum detectable difference at 80% statistical power. Detailed 95% confidence intervals for partial η_p^2 are provided in Table S4.

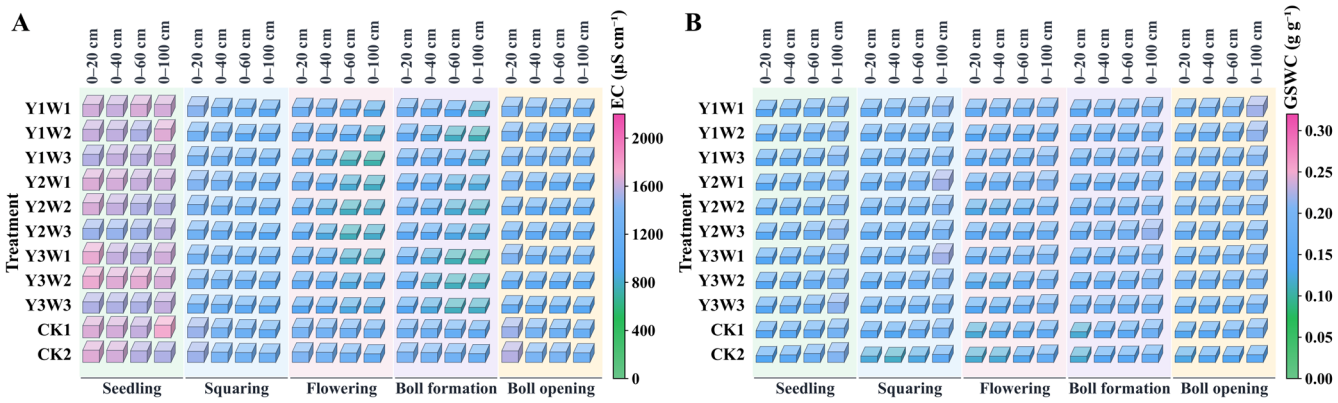


Figure 4. Seasonal variation in nested cumulative-profile electrical conductivity (EC; (**A**)) and gravimetric soil water content (GSWC; (**B**)) across the 11 treatments. Values are shown for the 0–20, 0–40, 0–60, and 0–100 cm cumulative profiles at five cotton growth stages. Each prism represents the treatment mean of three independent plots ($n = 3$), with colour indicating the magnitude of EC or GSWC.

3.2. Post-Harvest Bulk Density Responded Across Amendment Treatments

Post-harvest bulk density showed similar response patterns at both soil depths (Figure 5). CK1 and CK2 did not differ significantly (0–20 cm: t = −1.71, $p = 0.103$; 20–40 cm: t = −0.73, $p = 0.476$; df = 20), whereas the mean of the nine Y1W1–Y3W3 combinations was lower than CK1 at both depths (by 0.034 and 0.019 g cm^{-3} at 0–20 and 20–40 cm; t = −4.64, $p < 0.001$ and t = −2.69, $p = 0.014$, respectively; Table S5). All nine combinations also had lower bulk density than CK2, with reductions ranging from 1.78% to 5.08% at 0–20 cm. At 20–40 cm, the corresponding reductions ranged from 0.66 to 3.29% relative to CK2. Because comparisons with CK2 combine the effects of irrigation-water type and amendment, amendment effects are inferred from the contrasts with CK1. Across the nine Y1W1–Y3W3 combinations, bulk density was affected primarily by organic fertiliser rate (Y). Bulk density responded significantly to Y, but not to inoculant rate (W) or Y × W (Y: $p < 0.001$ at both depths; W: $p = 0.173$ and 0.253; Y × W: $p = 0.997$ and 0.983 at 0–20 and 20–40 cm, respectively; df = 2, 16 for Y and W and 4, 16 for Y × W; Table S5). The response to Y was non-monotonic: orthogonal contrasts confirmed a significant quadratic Y response at both depths (q = 0.0005 and 0.0003), and Y2 differed significantly from Y3 (q = 0.0219 and 0.0066), indicating that bulk density decreased from Y1 to Y2 and then partially increased at Y3. Among the individual combinations, Y2W2 had the lowest observed values, averaging 1.440 and 1.470 g cm^{-3} at 0–20 and 20–40 cm, respectively, corresponding to reductions of 4.00% and 2.84% relative to CK1, and of 5.08% and 3.29% relative to CK2. Thus, the intermediate Y level produced the lowest observed bulk density within the tested range, but this pattern should not be interpreted as evidence of a unique optimum rate. Relative to

the marginal mean of Y3W1, Y3W2, and Y3W3, bulk density under Y2W2 was 1.75% lower at 0–20 cm and 1.78% lower at 20–40 cm. These descriptive comparisons are distinct from the planned Y2–Y3 marginal contrasts and do not establish a unique optimum.

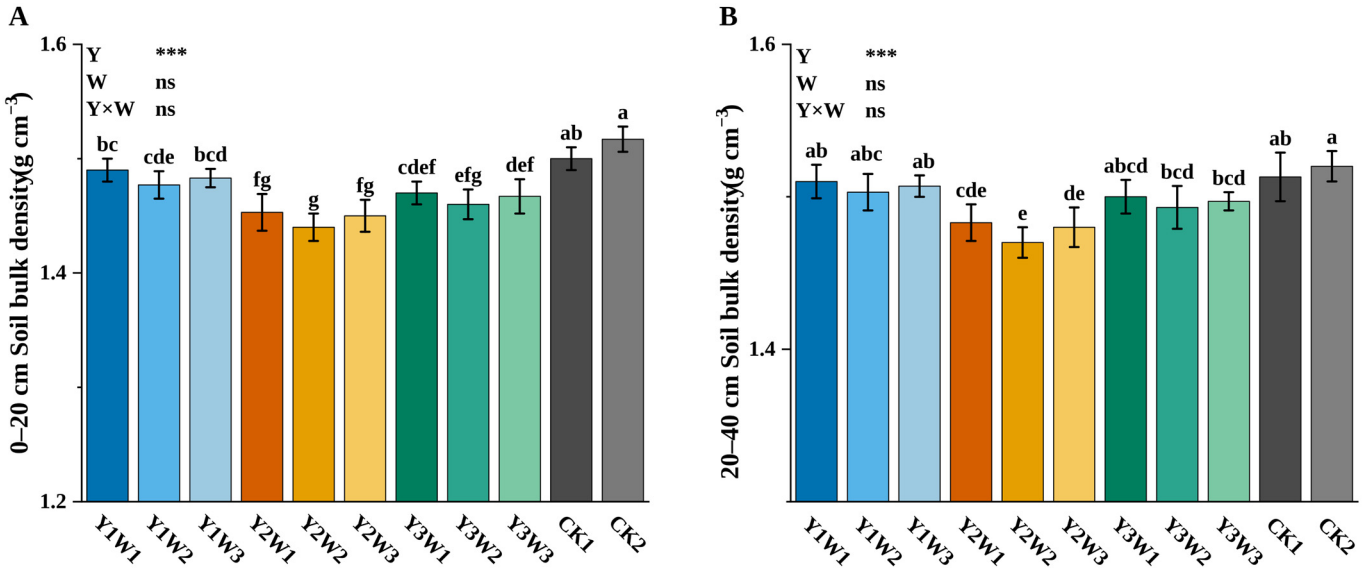


Figure 5. Post-harvest soil bulk density in the 0–20 cm (**A**) and 20–40 cm (**B**) layers across the eleven treatments. Bars are treatment means of three plots; error bars are standard deviations; different letters indicate differences among treatments at $p < 0.05$ (Duncan). Y, organic fertiliser rate; W, microbial inoculant rate; Y × W, their interaction. *** indicates $p < 0.001$, and ns indicates a non-significant effect ($p \geq 0.05$).

3.3. Microbial Assemblage Responses to Amendment Factors

Family-level composition varied among treatments in both microbial domains (Figure 6). In the bacterial assemblage, taxa grouped as Other accounted for 46.1–51.2% of the mean relative abundance across treatments. Among the individually displayed families, Thermoanaerobaculaceae and Vicinamibacteraceae had the highest overall mean relative abundances, at 5.55% and 5.37%, respectively, followed by Pseudomonadaceae (3.94%) and Sphingomonadaceae (3.55%). The fungal assemblage was dominated by Nectriaceae, Bulleribasidiaceae, and Pseudeurotiaceae, with overall mean relative abundances of 23.05%, 17.12%, and 15.20%, respectively.

Block-restricted PERMANOVA of CLR-transformed compositions confirmed significant treatment effects on both bacterial (pseudo-F = 4.74, $R^2 = 0.460$, $p = 0.0001$) and fungal (pseudo-F = 3.46, $R^2 = 0.447$, $p = 0.0001$) assemblages. Within the nine factorial treatments, bacterial assemblage composition responded significantly to Y (pseudo-F = 3.97, $R^2 = 0.116$, $p = 0.0021$), W (pseudo-F = 3.24, $R^2 = 0.095$, $p = 0.007$), and Y × W (pseudo-F = 2.94, $R^2 = 0.173$, $p = 0.001$). Corresponding effects were also detected for the fungal assemblage (Y: pseudo-F = 2.99, $R^2 = 0.095$, $p = 0.0004$; W: pseudo-F = 4.16, $R^2 = 0.132$, $p = 0.0001$; Y × W: pseudo-F = 3.20, $R^2 = 0.203$, $p = 0.0001$). Degrees of freedom were 10, 20 for the treatment effect, 2, 16 for Y and W, and 4, 16 for Y × W (Tables S6 and S7).

After Benjamini–Hochberg correction for multiple testing, family-level responses remained taxon-specific (Tables S6 and S7). Eleven of the twenty dominant bacterial families and ten of the twenty dominant fungal families showed at least one significant factorial effect ($q < 0.05$); results for all families, including non-significant ones, are given in Tables S6 and S7. Among bacteria, Rhodocyclaceae and Desulfuromonadaceae responded to Y, W, and Y × W, whereas Sphingomonadaceae showed significant Y and Y × W effects. Sphingomonadaceae reached its highest relative abundance under Y3W3 (4.81%), while

Rhodocyclaceae showed contrasting responses to increasing W among Y levels, consistent with its significant Y × W interaction. Bacillaceae, the family that includes the applied inoculant species, was among the 20 dominant bacterial families (mean relative abundance 1.48%) and responded to Y ($F = 9.39$, $q = 0.013$) and W ($F = 5.50$, $q = 0.042$) but not to Y × W ($F = 2.10$, $q = 0.193$); its mean relative abundance nevertheless remained between 1% and 2% in all 11 treatments, including the two non-inoculated controls (Figure 6A). Among fungi, Pucciniaceae responded to Y, W, and Y × W, whereas Chaetomiaceae and Cladosporiaceae showed factor-specific responses; interaction effects were also detected for Pseudeurotiaceae, Aspergillaceae, and Plectosphaerellaceae. Chaetomiaceae reached its highest relative abundance under Y1W3 (6.40%). Overall, amendment-rate effects were evident at both assemblage and dominant-family levels, with significant Y × W interactions in both microbial domains.

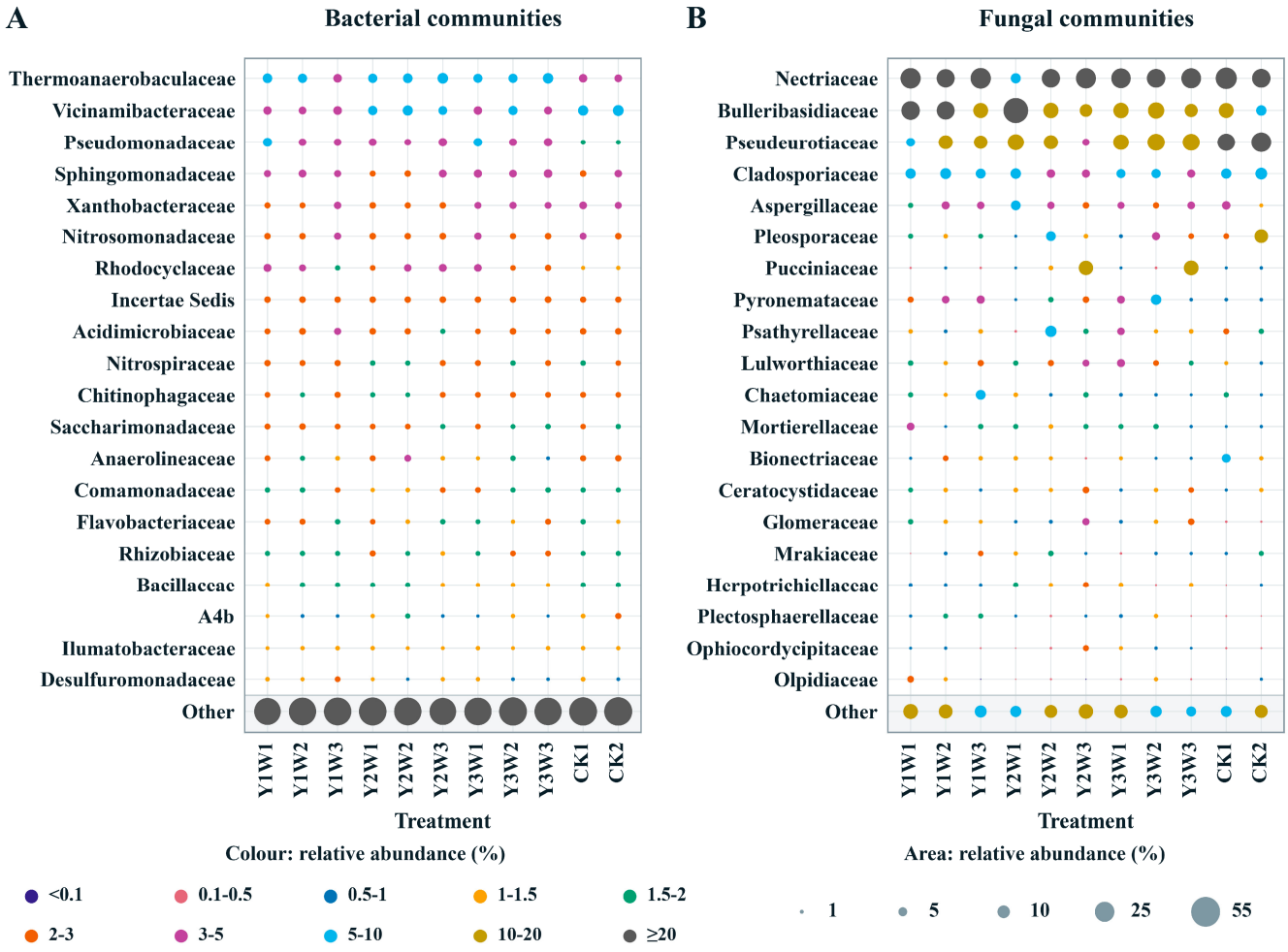


Figure 6. Family-level relative abundance of boll-stage root-zone bacterial (**A**) and fungal (**B**) assemblages across the eleven treatments. The 20 most abundant families in each microbial domain are shown individually, with all remaining families combined as Other. Bubble colour denotes relative-abundance classes, and bubble area is proportional to relative abundance (%).

3.4. Leaf Gas Exchange and Yield Formation Showed Trait-Specific Responses to Amendment Rates

At the boll stage, CK1 had numerically higher Pn, Tr, and Gs and lower Ci than CK2 (Figure 7A–D). Across the nine Y1W1–Y3W3 combinations, relative to CK1, Pn, Tr, and Gs were 0.33–14.04%, 1.51–20.13%, and 5.21–27.84% higher, respectively, whereas Ci changed by −12.25% to 3.56%. Factorial responses differed among gas-exchange traits: Pn was affected by both Y ($F = 13.09$, $p = 0.0004$) and W ($F = 6.55$, $p = 0.008$), and Tr also showed significant

overall responses to both Y ($F = 9.31$, $p = 0.002$) and W ($F = 5.05$, $p = 0.020$), whereas Gs showed no significant main effect ($p \geq 0.469$). For Ci, overall Y ($F = 3.81$, $p = 0.044$) and W ($F = 4.34$, $p = 0.031$) effects were detected, but none of the planned dose contrasts remained significant after BH adjustment. Orthogonal contrasts further showed linear and quadratic Y responses and a quadratic W response for Pn (q = 0.0055 for each), whereas the response of Tr was primarily characterised by a positive linear Y component (q = 0.007). No Y × W interaction was detected for any gas-exchange trait ($p \geq 0.503$; df = 2, 16 for Y and W and 4, 16 for Y × W; Table S8).

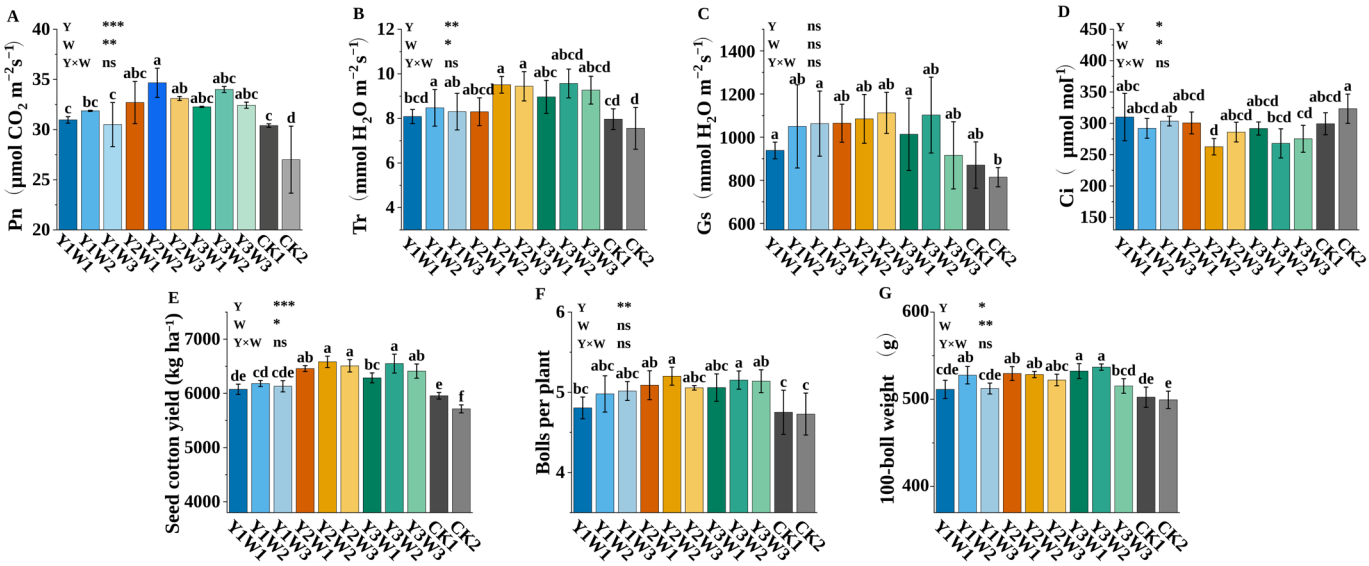


Figure 7. Boll-stage cotton leaf gas exchange and final yield formation across the eleven treatments: net photosynthetic rate (Pn; (**A**)), transpiration rate (Tr; (**B**)), stomatal conductance (Gs; (**C**)), intercellular CO_2 concentration (Ci; (**D**)), seed cotton yield (**E**), bolls per plant (**F**), and 100-boll weight (**G**). Bars are treatment means of three plots; error bars are standard deviations; different letters indicate differences among treatments at $p < 0.05$ (Duncan). Y, organic fertiliser rate; W, microbial inoculant rate; Y × W, their interaction. *, **, and *** indicate statistical significance at $p < 0.05$, $p < 0.01$, and $p < 0.001$, respectively; ns indicates a non-significant effect ($p \geq 0.05$).

Seed cotton yield and its components also differed among treatments (Figure 7E–G). Yield was 4.24% higher under CK1 than CK2 and 6.33–15.19% higher across the nine Y1W1–Y3W3 combinations than under CK2, with the highest value under Y2W2 (15.19% above CK2 and 10.51% above CK1). Within the factorial treatments, yield was affected by Y ($F = 31.00$, $p < 0.001$) and W ($F = 5.23$, $p = 0.018$) but not by Y × W ($F = 0.48$, $p = 0.747$; Table S8). Bolls per plant were also highest under Y2W2, 9.99% above CK2, and were mainly affected by Y but not by W (Y: $F = 9.21$, $p = 0.002$; W: $F = 3.48$, $p = 0.056$). In contrast, 100-boll weight reached its maximum under Y3W2, 7.51% above CK2, and was affected by both Y and W (Y: $F = 5.33$, $p = 0.017$; W: $F = 7.69$, $p = 0.005$). Yield showed both linear and quadratic responses to Y (q = 0.0001 for each) and a quadratic response to W (q = 0.018). However, the Y2–Y3 yield contrast was not significant (100.47 kg ha^{-1}, equivalent to 1.57% of the Y3 marginal mean; q = 0.088). The mean yield under Y2W2 was 2.60% higher than the Y3 marginal mean and only 0.50% higher than under Y3W2, indicating that the highest observed yield under Y2W2 does not establish an optimum application rate. Consistently, the exploratory response-surface model identified significant curvature in the yield response (quadratic Y term: $p = 0.005$, q = 0.019) but was used only to characterise the response pattern rather than to estimate an optimum (Table S9).

3.5. Associations of Bacterial and Fungal Assemblages with Soil and Crop Variables

Mantel analysis indicated positive correlations of bacterial assemblage composition with boll-stage 0–20 cm GSWC (Mantel r = 0.170, $p = 0.0062$) and seed cotton yield (Mantel r = 0.193, $p = 0.0031$). However, neither association remained statistically significant after BH adjustment across all 18 tests (q = 0.0558 for both; Figure 8). No fungal association remained significant after multiple-testing correction.

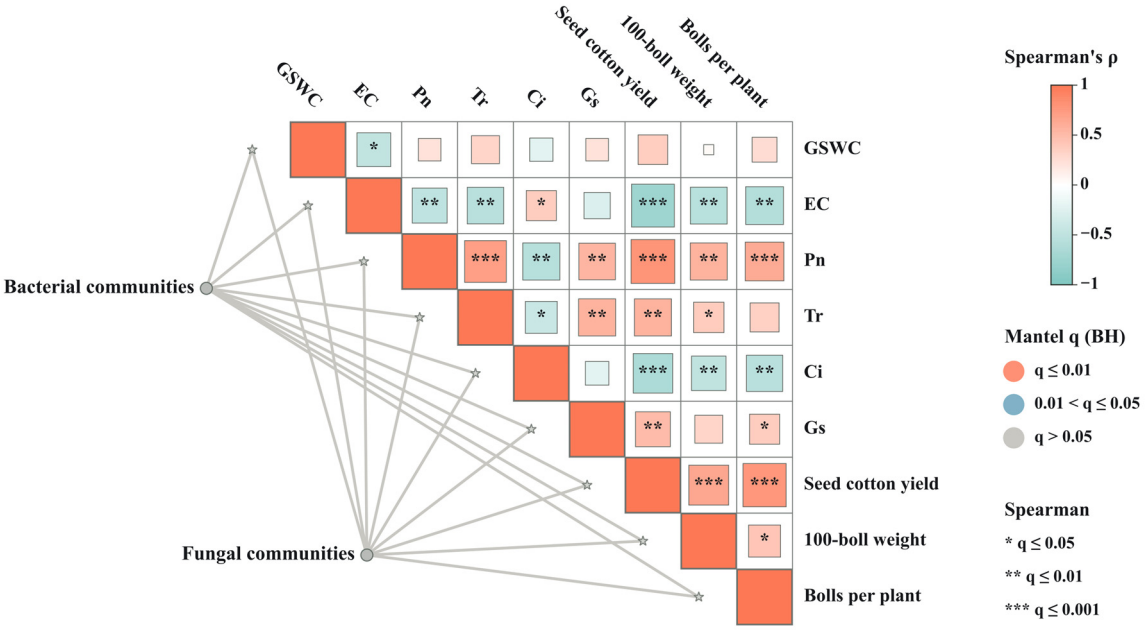


Figure 8. Mantel associations of the dominant bacterial and fungal family assemblages with boll-stage 0–20 cm GSWC and EC, leaf gas exchange, and yield-related traits, overlaid on a Spearman correlation matrix of the same soil and crop variables.

Spearman analysis further showed that GSWC was negatively correlated with EC. EC was negatively associated with Pn, Tr, seed cotton yield, 100-boll weight, and bolls per plant, but positively associated with Ci. Seed cotton yield was positively correlated with Pn, Tr, Gs, 100-boll weight, and bolls per plant, and negatively correlated with Ci and EC.

4. Discussion

4.1. GSWC and EC Showed Distinct Stage–Depth Responses and Detection Precision

The significant interactions with Stage and Depth indicate that amendment effects on GSWC and EC depended strongly on crop development and soil position rather than being uniformly expressed throughout the 0–100 cm profile. Both variables showed pronounced stage- and depth-dependent responses, but their spatiotemporal patterns differed. This distinction is consistent with the processes represented by the two measurements. Soil water content can respond locally to water retention, redistribution, and root uptake, whereas EC measured in a 1:5 soil–water extract reflects the combined outcome of ion dissolution, mobilisation, redistribution, concentration, and leaching [22,23]. Consequently, changes in soil water and extractable salts need not coincide in magnitude, timing, or soil depth even under the same irrigation-amendment regime.

The distinction between GSWC and EC was clearer in detection precision than in overall standardised effect magnitude. The Y and Y × W effects were broadly comparable between the two variables, whereas the W effect was more pronounced for GSWC. More consistently, GSWC showed lower residual variation and a lower minimum detectable difference, indicating greater precision in resolving amendment-rate variation. In contrast,

the higher variability of EC reduced the precision with which differences among amendment rates could be distinguished. This should not be interpreted as evidence that salinity-related processes were unimportant or that EC was intrinsically less responsive. Under film-mulched drip irrigation, soluble ions can be redistributed over relatively short spatial and temporal scales during repeated wetting and drying cycles, and EC therefore integrates several concurrent processes whose effects may partly offset one another [2–4].

The common magnetised–ionised water background provides a plausible physical context for these contrasting responses. Magnetic or magnetoelectric treatment has been reported to modify water molecular association and wetting-related properties, including surface tension, viscosity, and contact angle, which may influence infiltration, wetting-front behaviour, and subsequent water–salt redistribution [10,11,13]. Field applications in saline–alkali cotton systems have likewise reported changes in soil water distribution and salt movement under magnetised irrigation [10–12]. In the present experiment, the treated irrigation water also served as the carrier for repeated applications of the water-soluble organic fertiliser and microbial inoculant. Its movement therefore influenced the initial distribution of amendment-derived solutes within the wetted soil volume, while subsequent organic inputs may have further modified soil aggregation, pore organisation, and water-retention characteristics [24–26]. The *Bacillus subtilis* inoculant is less likely to exert a direct hydraulic effect, but may influence rhizosphere conditions indirectly through microbial activity, nutrient transformation, and root–soil interactions [16,27]. These processes could operate in a coupled manner, whereby irrigation-water movement governs the delivery and redistribution of water, amendments, and dissolved ions, while amendment-induced changes in the soil and rhizosphere subsequently affect water retention and ion redistribution. At key post-amendment stages, the clearer differences between the factorial treatments and CK1 than between CK1 and CK2 are consistent with an additional amendment-associated modification of water–salt conditions under the common magnetised–ionised water background. Because irrigation-water type was not factorially crossed with Y and W, however, this interpretation represents a plausible coupled process rather than a directly demonstrated synergistic interaction. Overall, GSWC resolved amendment-rate variation with greater precision, whereas EC reflected a more heterogeneous redistribution of extractable salts across growth stages and soil depths.

4.2. Taxon-Specific and Combination-Dependent Responses of Bacterial and Fungal Assemblages

Both bacterial and fungal assemblages responded significantly to Y, W, and Y × W, indicating that amendment-rate effects extended beyond individual taxa to the overall community composition. In both microbial domains, the Y × W interaction accounted for a larger proportion of compositional variation than either main effect alone, suggesting that community responses depended strongly on amendment-rate combinations rather than following simple dose-dependent trajectories [7,28].

Among bacteria, Rhodocyclaceae and Desulfuromonadaceae responded to Y, W, and Y × W, whereas Sphingomonadaceae showed significant Y and Y × W effects. Members of Sphingomonadaceae have been reported to possess broad capacities for the utilisation of soluble and aromatic carbon compounds [29], while members of Rhodocyclaceae and Desulfuromonadaceae have been associated with redox-sensitive environments and transformations [30,31]. These reported ecological characteristics provide plausible context for the observed compositional shifts, but family-level amplicon data do not demonstrate corresponding functional changes in the present field experiment. In particular, the contrasting response of Rhodocyclaceae to increasing W across different Y levels is more consistent with a combination-dependent redistribution of bacterial composition than with uniform enrichment as amendment input increased. Comparable restructuring of bacterial commu-

nities following *Bacillus subtilis* application has also been reported in saline–alkali cotton soils [16], providing context for the bacterial compositional shifts observed here. In the present study, both bacterial and fungal assemblages showed significant responses to Y, W, and Y × W, while family-level responses remained taxon-specific. Accordingly, counts of significant families do not provide a formal basis for comparing responsiveness between bacteria and fungi, and the observed bacterial compositional shifts should not be taken as evidence for establishment of the applied *B. subtilis* strain. Consistent with this caution, the relative abundance of Bacillaceae lay within the same range (1–2%) in inoculated and non-inoculated plots (Figure 6A; Table S6).

Fungal responses were likewise taxon-specific and frequently interaction-dependent. Pucciniaceae responded to Y, W, and Y × W, whereas Chaetomiaceae and Cladosporiaceae showed factor-specific responses; Pseudeurotiaceae, Aspergillaceae, and Plectosphaerellaceae also exhibited significant interaction effects. Members of Chaetomiaceae have been reported among saprotrophic fungi associated with organic-matter turnover in agricultural soils [32,33], whereas Plectosphaerellaceae includes plant-associated species with diverse ecological roles [34,35]. Pucciniaceae comprises obligately biotrophic rust fungi [36], but family-level ITS data cannot resolve species identity, host association, or ecological activity in the present soil samples. Thus, these taxonomic associations provide ecological context rather than direct evidence of functional change. More broadly, differences in resource acquisition and substrate utilisation between bacterial and fungal communities may contribute to the distinct taxon-specific response patterns observed here [17]. Overall, amendment rates reorganised both bacterial and fungal assemblages, with much of the response expressed through taxon-specific and combination-dependent changes rather than uniform shifts across the microbial community.

4.3. Coordinated Soil–Plant Responses and Their Covariation

Amendment-rate effects were expressed across soil physical condition, crop physiology, and final yield formation, but these responses occurred at different stages of the season and should not be interpreted as a single causal sequence. Post-harvest bulk density provided an end-of-season physical response that was more closely associated with organic fertiliser rate. Given the relatively small amount of organic material added relative to the mass of the cultivated soil layer, the observed response is unlikely to reflect direct organic-matter addition alone. Organic inputs can promote aggregation and root development, while root proliferation, rhizodeposition, and root-derived biopores can further modify soil structural organisation [24,26,37]. Root-mediated effects on aggregation and pore architecture are well established in the broader soil-structure literature [38,39]. These processes therefore provide plausible explanations for the observed physical response, but they were not directly measured here. Moreover, bulk density was determined only after mechanical harvest; although visible wheel tracks were avoided, spatial heterogeneity, soil water status at sampling, and machinery-related disturbance may also have contributed to the observed variation. Bulk density is therefore interpreted as a complementary post-harvest physical endpoint rather than as direct evidence of a specific soil structural mechanism.

The physiological and agronomic measurements provide a complementary view of the soil–plant response. Changes in root-zone water, salinity, and resource availability can influence root activity, nutrient acquisition, and plant carbon assimilation, while organic amendments and microbial inoculation may further modify rhizosphere resource turnover and plant stress responses [16,27]. Consistent with this framework, lower EC coincided with stronger photosynthetic performance and greater yield formation, whereas yield covaried positively with several photosynthetic traits and yield components [40,41]. These relationships suggest coordinated variation between root-zone conditions and crop performance

rather than a response governed by a single soil property [42,43]. They also help explain why increasing amendment input did not produce proportional changes across all measured traits: physical soil condition, leaf physiological status, and reproductive development integrate management effects through different processes and over different temporal scales. Because bulk density was measured after harvest and was not included in the correlation analysis, it should be viewed as complementary to, rather than mechanistically linked with, the boll-stage physiological relationships.

The microbial results add a biological dimension to this coordinated response. The exploratory covariation of bacterial assemblage composition with GSWC and yield may reflect shared responses to changes in the root-zone environment rather than a direct microbial pathway to crop performance. Variation in soil water status, salinity, and organic-resource supply can simultaneously affect plant activity, root-derived carbon inputs, and microbial habitats, while rhizodeposition provides an important interface linking roots, soil structure, and microbial resource availability [37,44,45]. Bacterial assemblages may respond relatively rapidly to changes in labile substrates and rhizosphere conditions, whereas fungal assemblages may integrate different or more slowly varying resource pools [17,46]. This provides a plausible ecological context for the observed association patterns, but does not establish that bacterial restructuring mediated the crop response or that bacterial and fungal coupling differed statistically. Moreover, block-restricted Mantel permutations do not remove covariation jointly induced by treatment. The microbial associations are therefore most appropriately interpreted as parallel biological responses within the same soil–plant environment. Taken together, the physical, physiological, biological, and agronomic measurements indicate that amendment-rate effects were coordinated across system components, but were expressed through different processes and at different temporal scales.

4.4. Implications for Evaluating Amendment-Rate Responses in Saline–Alkali Cotton Systems

The different response patterns of GSWC, EC, bulk density, microbial composition, and crop traits indicate that amendment-rate effects cannot be characterised adequately by a single endpoint. EC remains essential for describing soil salt status, and its standardised responses to amendment rate were broadly comparable in magnitude to those of GSWC. Its greater residual variability, however, reduced the precision with which differences among rates could be resolved. This does not establish lower intrinsic responsiveness. Evaluation should therefore combine extract EC with complementary physical, biological, and agronomic measurements, while retaining the distinction between response magnitude and detection precision.

Bulk density provides one such complementary physical endpoint. Its response to organic fertiliser rate shows that amendment-rate effects were also expressed in post-harvest soil physical condition, a component of the system that EC does not describe. Bulk density and EC therefore provide complementary information on physical condition and salt status, respectively. More generally, the combined responses of GSWC, EC, bulk density, microbial assemblages, leaf gas exchange, and yield demonstrate the value of evaluating amendment rates across multiple system components rather than assigning disproportionate importance to any single measurement.

A further implication is that responses were not consistently proportional to increasing amendment input within the tested range. Physical, microbial, physiological, and yield-related traits showed non-linear, factor-specific, or combination-dependent patterns, and favourable responses were not uniformly concentrated at the highest input levels. Similar non-linear responses to *Bacillus subtilis* application rate have been reported in related saline–alkali cotton systems [5,47]. Within the narrow rate range, single site, and single season examined here, these findings caution against assuming a simple proportional

dose–response relationship, but they do not by themselves support a general conclusion about the relationship between input level and benefit. Intermediate-rate combinations that perform favourably across several complementary endpoints may therefore provide useful candidates for subsequent agronomic validation.

4.5. Limitations

Several limitations define the scope of inference from this study. First, soil water was quantified as gravimetric soil water content (GSWC) across seven soil layers rather than as volumetric water content or soil water storage. Because bulk density was measured only after harvest, seasonal soil water storage could not be reconstructed reliably. In addition, the absence of field water-balance or evapotranspiration measurements prevents separation of treatment-related differences in soil water status arising from redistribution and storage from those associated with crop water use. Moreover, EC was measured in a 1:5 soil–water extract and therefore represents extract conductivity rather than in situ soil-solution salinity; it also does not resolve responses in individual ions, exchangeable sodium, sodium adsorption ratio (SAR), or osmotic stress. Because ESP and SAR were not determined at baseline, the description of the site as saline–alkali rests on EC and pH alone, and its sodicity status is unknown.

Second, the experiment was conducted at one site over one growing season. Only three non-zero rates of each amendment were tested, and no organic-fertiliser-only or inoculant-only treatments were included, so that the separate contribution of each amendment relative to the unamended control cannot be isolated. Because the organic fertiliser also supplied mineral nutrients, its rate effects cannot be attributed to organic matter alone. Orthogonal linear and quadratic contrasts and the exploratory response-surface analysis characterise response curvature within the tested range, but they do not establish a unique agronomic optimum. The observed amendment-rate responses, including the non-linear responses of bulk density, gas exchange, and yield-related traits, therefore require validation across years and saline–alkali environments before they can support general rate recommendations. Leaf gas exchange was likewise measured on a single date and on one leaf per plot, without documented cuvette conditions, so that these data indicate relative treatment differences under the prevailing conditions rather than standardised photosynthetic capacity.

Third, microbial sampling was restricted to the 0–20 cm layer at the boll stage. The bacterial and fungal results consequently represent a stage-specific compositional snapshot rather than seasonal or vertical community dynamics. Assemblage analyses were based on the 20 dominant families plus an aggregated Other category. Although CLR transformation accounted for the compositional nature of the data, amplicon sequencing provides relative taxonomic composition rather than absolute abundance, microbial activity, or process rates, and establishment of the applied *Bacillus subtilis* strain was not directly verified; no carrier-only or autoclaved-inoculant control was included, so that inoculant-rate effects refer to the formulated product rather than to viable cells alone, and the soluble-salt load of the two commercial products was not quantified. Moreover, block-restricted Mantel permutations control field-block structure but do not remove covariation jointly induced by treatment. The resulting assemblage–environment associations should therefore be interpreted as covariation rather than microbial mediation, and differences in statistical significance between bacterial and fungal assemblages do not constitute a direct test of domain-level differences. Formal residual diagnostics for the family-level models and separate tests of multivariate dispersion for PERMANOVA were not conducted. Therefore, microbial results are interpreted cautiously as treatment-associated compositional responses within this dataset.

Fourth, the nine Y1W1–Y3W3 combinations were established only under magnetised–ionised water irrigation. Effects of organic fertiliser rate and inoculant rate are therefore conditional on this irrigation background, and interactions between irrigation-water type and amendment rate cannot be resolved from the present design. The CK1–CK2 comparison provides a reference for the irrigation-water contrast but does not substitute for a fully crossed irrigation × amendment experiment. In addition, irrigation-water quality (EC, pH, and major ions) and the properties of the water before and after magnetoelectric treatment were not measured, so that the extent to which the treatment altered the irrigation water in this experiment cannot be verified.

Finally, bulk density was measured only once, immediately after mechanical harvest, and no plot-level pre-treatment bulk-density measurements were available for paired comparison. Cores were collected beneath cotton plants and outside visible machinery wheel tracks, but soil water status at sampling was not recorded, and residual spatial heterogeneity or machinery-related effects cannot be excluded. Root traits, aggregate stability, pore architecture, infiltration, and soil water-retention characteristics were also not measured. Bulk density is therefore interpreted as a post-harvest physical endpoint associated with organic fertiliser rate in this experiment, rather than evidence that structural change caused the seasonal GSWC patterns.

Future work should prioritise multi-season and multi-site validation together with paired measurements of soil physical condition, root traits, aggregate stability, infiltration, and soil water retention. Measurements of volumetric soil water, crop water use, and soluble-ion composition, including derived SAR, would help resolve the processes underlying the observed water–salt responses. Repeated microbial sampling across growth stages and soil depths, together with absolute abundance, verification of inoculant establishment, and selected functional measurements, would further clarify whether compositional shifts are accompanied by changes in microbial abundance or activity.

5. Conclusions

This study demonstrates that amendment-rate responses in saline–alkali cotton were dependent on growth stage, soil depth, and system component within the magnetised–ionised water irrigation background. GSWC and EC showed distinct temporal and depth-dependent response patterns differing more in detection precision than in standardised effect magnitude. Soil physical, microbial, physiological, and agronomic responses were likewise not uniformly proportional to increasing amendment input, and bacterial assemblage composition showed exploratory covariation with boll-stage GSWC and seed cotton yield. These findings indicate that amendment-rate evaluation should integrate multiple components of the soil–microbe–crop system rather than rely on a single endpoint. Within the tested range, Y2W2 showed favourable performance across several measured responses, but the present single-season, single-site experiment does not establish a unique agronomic optimum. Y2W2 should therefore be considered a promising candidate for multi-season and multi-site validation before broader agronomic recommendation or commercial application.

Supplementary Materials: The following supporting information can be downloaded at: https://www.mdpi.com/article/10.3390/agriculture16212356/s1, Table S1: AIC comparison of candidate temporal covariance structures for GSWC and EC.; Table S2: Depth effects and amendment-rate × depth interactions for GSWC and EC; Table S3: Planned contrasts for GSWC and EC between irrigation controls and amendment treatments; Table S4: Baseline-adjusted stage- and layer-specific effects of organic fertiliser and inoculant rates on GSWC and EC; Table S5: Post-harvest soil bulk density and dose-response statistics; Table S6: Bacteria assemblage- and family-level responses to amendment factors; Table S7: Fungi assemblage- and family-level responses to amendment factors; Table S8: Factorial and

dose-response effects on leaf gas exchange, seed cotton yield and yield components; Table S9: Exploratory response-surface analyses of leaf gas exchange and yield-related responses.

Author Contributions: H.W.: conceptualisation, investigation, data curation, software, validation, visualisation, writing—original draft. Z.M.: conceptualization, methodology, formal analysis. Y.X.: methodology, formal analysis. Q.F.: project administration, funding acquisition, supervision, writing—review and editing, resources. S.L.: conceptualization, writing—review and editing. Z.S.: formal analysis, investigation. Y.Z.: methodology, investigation. Q.M.: methodology, investigation. Y.M.: conceptualization, formal analysis. Q.W.: methodology, formal analysis, supervision. All authors have read and agreed to the published version of the manuscript.

Funding: This study was funded by the Major Science and Technology Project of the Xinjiang Uygur Autonomous Region (No. 2024A03007-5, 2024A03007-4, and 2023A02002-5), the Natural Science Foundation of Xinjiang Uygur Autonomous Region, the Project of Xinjiang Uygur Autonomous Region Eco-Hydraulic Research Center (Academician and Expert Workstation of the Water Resources Department of Xinjiang Uygur Autonomous Region) (2024.D-002), and the Open Research Fund Program of Xinjiang Key Laboratory of Hydraulic Engineering Security and Water Disasters Prevention (ZDSYS-YJS-2024-53).

Data Availability Statement: The raw 16S rRNA gene and ITS sequencing data are available in the NCBI Sequence Read Archive under BioProject accession number PRJNA1513417. Other data supporting the findings of this study are available from the corresponding authors upon reasonable request.

Conflicts of Interest: The authors declare that they have no known competing financial interests or personal relationships that could have appeared to influence the work reported in this paper.

References

1. Hu, Q.; Cao, H.; He, Z.; Shi, H.; Ren, Z.; Qi, C. Effects of leaching amounts and drip irrigation types on water-salt distribution and seed cotton yield in northern Xinjiang, China. *Field Crops Res*. **2025**, *328*, 109947. [CrossRef]
2. Liu, X.Q.; Li, M.Q.; Xue, D.; He, S.; Fan, J.L.; Zhang, F.C.; Yin, F.H. Optimal drip irrigation leaching amount and timing enhanced cotton fiber yield, quality and nitrogen uptake by regulating soil salinity and nitrate nitrogen in saline-alkaline fields. *J. Integr. Agric*. **2025**, *24*, 2389–2409. [CrossRef]
3. Xu, Y.B.; Xue, B.; Wang, J.R.; Meng, Q.; Dong, L.; Gong, P.; Li, P.F.; Dong, J.S.; Xia, H.J.; Liu, H.G.; et al. Effects of deep tillage and pre-irrigation on soil salinity, water use and performance of cotton in a saline soil. *Agric. Water Manag*. **2026**, *329*, 110351. [CrossRef]
4. Ma, Z.L.; Zhang, J.Z.; Li, W.H.; Ye, H.C.; Yin, F.H.; Wen, Y.; Wang, Z.H. The dual-threat: How saline water irrigation compromises soil health and seed cotton yield under mulched drip irrigation in Xinjiang, China. *Agric. Water Manag*. **2025**, *320*, 109847. [CrossRef]
5. Jiang, Z.B.; Wang, Q.J.; Ning, S.R.; Lin, S.D.; Hu, X.Q.; Song, Z.X. Application of Magnetized Ionized Water and Bacillus subtilis Improved Saline Soil Quality and Cotton Productivity. *Plants* **2024**, *13*, 2458. [CrossRef] [PubMed]
6. Xia, H.J.; Liu, H.G.; Gong, P.; Li, P.F.; Xu, Q.; Zhang, Q.; Yang, C.K.; Meng, Q. Applying bio-organic fertilizer improved saline alkaline soil properties and cotton yield in Xinjiang. *Sci. Rep*. **2025**, *15*, 13235. [CrossRef] [PubMed]
7. Tang, M.S.; Yang, J.; Yan, Z.; Fu, Q.P.; Wang, Z.F.; Lin, S.D.; Deng, M.J.; Wang, Q.J.; Ma, Z.H.; Ma, Y.J. Co-application of organic fertilizer and composite microbial inoculant improves soil quality and cotton yield in saline-alkaline cotton fields of southern Xinjiang. *Ind. Crops Prod*. **2026**, *248*, 123615. [CrossRef]
8. Jiang, Z.B.; Wang, Q.J.; Ning, S.R.; Hu, X.Q.; Yuan, S. Growth and Yield Response and Water Use Efficiency of Cotton under Film-Mulched Drip Irrigation to Magnetized Ionized Water and Bacillus subtilis in Saline Soil in Xinjiang. *Agronomy* **2023**, *13*, 1644. [CrossRef]
9. Song, J.S.; Zhang, H.Y.; Chang, F.D.; Yu, R.; Wang, J.; Chen, A.P.; Xu, Y.; Liu, Y.; Zhou, J.; Li, Y.Y. Subsurface organic amendment of a saline soil increases ecosystem multifunctionality and sunflower yield. *Sci. Total Environ*. **2024**, *917*, 170276. [CrossRef] [PubMed]
10. Duan, X.X.; Wang, Q.J.; Mu, W.Y.; Ma, C.K.; Wei, K.; Sun, Y.; Zhao, X. Optimizing brackish water irrigation using magnetoelectric treatment for sustainable cotton cultivation in the arid region of southern Xinjiang. *Agric. Water Manag*. **2025**, *318*, 109684. [CrossRef]
11. Yi, G.; Quanjiu, W.; Kang, W.; Jihong, Z.; Kai, W.; Yang, L. Spring irrigation with magnetized water affects soil water-salt distribution, emergence, growth, and photosynthetic characteristics of cotton seedlings in Southern Xinjiang, China. *BMC Plant Biol*. **2023**, *23*, 174. [CrossRef] [PubMed]

12. Xin, M.L.; Zhao, Q.; Qiao, Y.; Ma, Y.J. Magnetized Saline Water Drip Irrigation Alters Soil Water-Salt Infiltration and Redistribution Characteristics. *Water* **2024**, *16*, 2693. [CrossRef]
13. Moussa, M.; Zarai, B.; Hachicha, M. Magnetic water treatment: Theory and effects on treated water—A systematic review. *Euro-Mediterr. J. Environ. Integr.* **2025**, *10*, 2323–2342. [CrossRef]
14. Abdelsalam, H.; Mostafa, H.; El-Ansary, M.; Awad, M.; Sultan, W. Magnetization treatment effect on some physical and biological characteristics of saline irrigation water. *Sci. Rep.* **2025**, *15*, 19803. [CrossRef] [PubMed]
15. Řezáčová, V.; Czakó, A.; Stehlík, M.; Mayerová, M.; Šimon, T.; Smatanová, M.; Madaras, M. Organic fertilization improves soil aggregation through increases in abundance of eubacteria and products of arbuscular mycorrhizal fungi. *Sci. Rep.* **2021**, *11*, 12548. [CrossRef] [PubMed]
16. Xia, H.J.; Liu, H.G.; Gong, P.; Li, P.F.; Xu, Q.; Zhang, Q.; Sun, M.Y.; Meng, Q.; Ye, F.H.; Yin, W.Z. Study of the mechanism by which Bacillus subtilis improves the soil bacterial community environment in severely saline-alkali cotton fields. *Sci. Total Environ.* **2025**, *958*, 178000. [CrossRef] [PubMed]
17. Wang, C.Q.; Kuzyakov, Y. Mechanisms and implications of bacterial–fungal competition for soil resources. *ISME J.* **2024**, *18*, wrae073. [CrossRef] [PubMed]
18. Bai, X.L.; Zhang, E.; Wu, J.M.; Ma, D.H.; Zhang, C.H.; Zhang, B.Y.; Liu, Y.P.; Zhang, Z.; Tian, F.; Zhao, H.; et al. Soil fungal community is more sensitive than bacterial community to modified materials application in saline–alkali land of Hetao Plain. *Front. Microbiol.* **2024**, *15*, 1255536. [CrossRef] [PubMed]
19. Zhang, G.L.; Bai, J.H.; Zhai, Y.J.; Jia, J.; Zhao, Q.Q.; Wang, W.; Hu, X.Y. Microbial diversity and functions in saline soils: A review from a biogeochemical perspective. *J. Adv. Res.* **2024**, *59*, 129–140. [CrossRef]
20. Bista, M.K.; Adhikari, B.; Sankarapillai, L.V.; Pieralisi, B.; Reddy, K.R.; Jenkins, J.; Bheemanahalli, R. Drought and heat stress induce differential physiological and agronomic trait responses in cotton. *Ind. Crops Prod.* **2024**, *222*, 119540. [CrossRef]
21. Lu, R.K. *Methods for Soil Agrochemical Analysis*; China Agricultural Science and Technology Press: Beijing, China, 2000.
22. Lin, D.; Bi, W.; He, Y.; Ge, Y.; Mao, X. Optimizing irrigation amount and salinity level for sustainable cotton production and soil health. *Agric. Water Manag.* **2025**, *316*, 109581. [CrossRef]
23. Kargas, G.; Petsetidi, A.P.; Londra, P.; Schillaci, C. Evaluation of different pedotransfer functions for the prediction of soil salinity using the electrical conductivity of the 1:5 soil:water extract (EC1:5). *Geoderma Reg.* **2026**, *46*, e01130. [CrossRef]
24. Ren, L.J.; Yang, H.; Li, J.; Zhang, N.; Han, Y.Y.; Zou, H.T.; Zhang, Y.L. Organic fertilizer enhances soil aggregate stability by altering greenhouse soil content of iron oxide and organic carbon. *J. Integr. Agric.* **2025**, *24*, 306–321. [CrossRef]
25. Pan, Y.; Wang, D.Y.; Tan, T.T.; An, J.; Jin, X.X.; Zou, H.T.; Zhang, Y.L.; Yu, N.; Siddique, K.H.M. Effect of organic amendments on soil organic carbon fractions, water retention, and mechanical properties in a Chinese Alfisol. *Soil Tillage Res.* **2025**, *254*, 106723. [CrossRef]
26. Skadell, L.E.; Dettmann, U.; Guggenberger, G.; Don, A. Effects of Agricultural Management on Water Retention via Changes in Organic Carbon in Topsoil and Subsoil. *J. Plant Nutr. Soil Sci.* **2025**, *188*, 949–963. [CrossRef]
27. Lei, Q.Y.; Bai, J.M.; Tao, W.H.; Yan, H.K.; Huo, Y.Z.; Deng, M.J.; Jiang, P.a.; Biswas, A. Synergistic regulation of cotton yield and quality formation by magnetoelectric brackish water drip irrigation and plant growth-promoting rhizobacteria in arid regions. *Agric. Water Manag.* **2026**, *332*, 110514. [CrossRef]
28. Cai, Z.; Shi, J.; Fu, S.; Li, F.; Lv, L.; Liu, Q.; Zhang, H.; Bao, S. Optimized fertilizer–microbe ratios enhance synergistic restoration of alpine mining ecosystems. *Front. Microbiol.* **2025**, *16*, 1709528. [CrossRef] [PubMed]
29. Fujita, M.; Hirano, R.; Nagayoshi, K.; Kamimura, N.; Masai, E. Uptake system of lignin-derived aromatic acids in promising Sphingomonadaceae strains for lignin valorization through biological funneling. *Sci. Rep.* **2025**, *15*, 23644. [CrossRef] [PubMed]
30. Wang, C.-N.; Masuda, Y.; Senoo, K. Ammonium-Generating Microbial Consortia in Paddy Soil Revealed by DNA-Stable Isotope Probing and Metatranscriptomics. *Microorganisms* **2025**, *13*, 1448. [CrossRef] [PubMed]
31. Kronberg, R.; Teikari, J.E.; Bore, E.; Kekkonen, H.; Kanerva, S.; Koskinen, M.; Karhu, K.; Seppänen, A.; Mattila, T.; Heinonsalo, J.; et al. Impact of Seasonal Waterlogging on Organic Carbon Stabilisation and Microbial Communities in Cultivated Mineral Soils. *Eur. J. Soil Sci.* **2026**, *77*, e70391. [CrossRef]
32. Mo, Y.J.; Bier, R.; Li, X.L.; Daniels, M.; Smith, A.; Yu, L.; Kan, J.J. Agricultural practices influence soil microbiome assembly and interactions at different depths identified by machine learning. *Commun. Biol.* **2024**, *7*, 1349. [CrossRef] [PubMed]
33. Oliveira, M.C.O.; Alves, A.; Fidalgo, C.; de Freitas, J.G.R.; Pinheiro de Carvalho, M.A.A. Variations in the structure and function of the soil fungal communities in the traditional cropping systems from Madeira Island. *Front. Microbiol.* **2024**, *15*, 1426957. [CrossRef] [PubMed]
34. Cui, Y.P.; Huang, F.; Guo, B.; Ling, J.F.; Wang, J.H.; Song, X.B. First Report of Coptis Wilt Caused by Plectosphaerella cucumerina in China. *Plant Dis.* **2024**, *108*, 2580. [CrossRef]
35. Zhao, Q.; Jia, A.; Yang, H.; Hu, J.; Gao, X.; Zhao, W.; Zhou, L.; Zhang, M.; Li, Z.; Zhang, W. Unveiling Species Diversity of *Plectosphaerellaceae* (*Sordariomycetes*) Fungi Involved in Rhizome and Root Rots of Ginger in Shandong Province, China. *Microorganisms* **2025**, *13*, 2180. [CrossRef] [PubMed]

36. Madhushan, A.; Weerasingha, D.B.; Ilyukhin, E.; Taylor, P.W.J.; Ratnayake, A.S.; Liu, J.-K.; Maharachchikumbura, S.S.N. From Natural Hosts to Agricultural Threats: The Evolutionary Journey of Phytopathogenic Fungi. *J. Fungi* **2025**, *11*, 25. [CrossRef] [PubMed]
37. Mueller, C.W.; Baumert, V.; Carminati, A.; Germon, A.; Holz, M.; Kögel-Knabner, I.; Peth, S.; Schlüter, S.; Uteau, D.; Vetterlein, D.; et al. From rhizosphere to detritusphere—Soil structure formation driven by plant roots and the interactions with soil biota. *Soil Biol. Biochem.* **2024**, *193*, 109396. [CrossRef]
38. Xiao, T.; Li, P.; Fei, W.; Wang, J. Effects of vegetation roots on the structure and hydraulic properties of soils: A perspective review. *Sci. Total Environ.* **2024**, *906*, 167524. [CrossRef] [PubMed]
39. Dimattia, B.G.; Righi, A.; Bettuzzi, M.; Koestel, J.; Morigi, M.P.; Brancaccio, R.; Salvi, S.; Hernandez-Soriano, M.C.; Bittelli, M. Root traits of different wheat cultivars influence soil structure: An X-ray computed tomography and root morphology study. *Geoderma* **2025**, *459*, 117349. [CrossRef]
40. Ma, Z.L.; Liu, J.; Wen, Y.; Zhang, J.Z.; Yin, F.H.; Guo, L.; Li, W.H.; He, J.; Ma, J.Y.; Liang, Y.H.; et al. Optimizing cotton yield through appropriate irrigation water salinity: Coordinating above- and below-ground growth and enhancing photosynthetic capacity. *Eur. J. Agron.* **2024**, *154*, 127095. [CrossRef]
41. Xiao, C.; Zhang, F.; Li, Y.; Fan, J.; Xu, X.; Liu, X. Optimal drip irrigation leaching amount and times enhance seed cotton yield and its stability by improving soil chemical environment and source-sink relationship. *Field Crops Res.* **2024**, *317*, 109531. [CrossRef]
42. Wang, X.; Cheng, L.; Xiong, C.; Whalley, W.R.; Miller, A.J.; Rengel, Z.; Zhang, F.; Shen, J. Understanding plan—Soil interactions underpins enhanced sustainability of crop production. *Trends Plant Sci.* **2024**, *29*, 1181–1190. [CrossRef] [PubMed]
43. Yu, N.; Alam, S.; Ren, B.; Zhao, B.; Liu, P.; Zhang, J. Long-term integrated soil-crop system management promoted rhizosphere nitrogen cycling and reduced N_2O emission of maize. *Field Crops Res.* **2024**, *319*, 109641. [CrossRef]
44. Li, H.; Chang, L.; Liu, H.; Li, Y. Diverse factors influence the amounts of carbon input to soils via rhizodeposition in plants: A review. *Sci. Total Environ.* **2024**, *948*, 174858. [CrossRef] [PubMed]
45. Witzgall, K.; Steiner, F.A.; Hesse, B.D.; Riveras-Muñoz, N.; Rodríguez, V.; Teixeira, P.P.C.; Li, M.; Oses, R.; Seguel, O.; Seitz, S.; et al. Living and decaying roots as regulators of soil aggregation and organic matter formation—From the rhizosphere to the detritusphere. *Soil Biol. Biochem.* **2024**, *197*, 109503. [CrossRef]
46. Philippot, L.; Chenu, C.; Kappler, A.; Rillig, M.C.; Fierer, N. The interplay between microbial communities and soil properties. *Nat. Rev. Microbiol.* **2024**, *22*, 226–239. [CrossRef] [PubMed]
47. Xia, H.J.; Liu, H.G.; Sun, K.; Gong, P.; Li, P.F.; Xu, Q.; Meng, Q.; Ye, F.H.; Sun, M.Y.; Xu, Y.B.; et al. Mechanisms of cotton growth and water use efficiency in saline-alkali soil using deep vertical rotary tillage and Bacillus subtilis. *Ind. Crops Prod.* **2026**, *239*, 122472. [CrossRef]

Disclaimer/Publisher's Note: The statements, opinions and data contained in all publications are solely those of the individual author(s) and contributor(s) and not of MDPI and/or the editor(s). MDPI and/or the editor(s) disclaim responsibility for any injury to people or property resulting from any ideas, methods, instructions or products referred to in the content.